Middle East Journal of Applied Science & Technology (MEJAST)
Volume 8, Issue 4, Pages 35-53, October-December 2025

Synergistic Hepatorenal Oxidative Injury from 28-Day Co-Exposure to Dichlorvos, Dimethoate, and Cypermethrin in Female Rats: Biochemical and Histopathological Evidence

Adeyemi, Oyeyemi[1*] & Emerure, Suzan Uyoyouoghene[2]

[1,2]*Department of Environmental Management and Toxicology, Federal University of Petroleum Resources, Effurun, Nigeria.*
Corresponding Author (Adeyemi, Oyeyemi) Email: adeyemi.oyeyemi@fupre.edu.ng[*]

DOI: https://doi.org/10.46431/mejast.2025.8403

Article Received: 08 September 2025 *Article Accepted: 13 November 2025* *Article Published: 16 November 2025*

ABSTRACT

This study evaluated the oxidative stress response and histopathological alterations in liver and kidney tissues of rats exposed to dichlorvos, dimethoate, cypermethrin, and their combinations over 28 days. Malondialdehyde (MDA) levels, catalase (CAT), and superoxide dismutase (SOD) activities were assessed as biomarkers of lipid peroxidation and antioxidant defence, alongside histological examinations. Liver MDA concentrations significantly increased from 3.2 nmol/g in control (Group A) to 7.5 nmol/g in the triple combination group (Group H), indicating severe lipid peroxidation. Similarly, kidney MDA levels rose from 2.9 nmol/g (Group A) to 7.3 nmol/g (Group H), confirming systemic oxidative stress. CAT activity in liver tissues increased progressively, with Group H recording the highest activity at 0.125 ± 0.002 U/mg protein compared to 0.045 ± 0.002 U/mg in the control. In the kidney, CAT activity escalated from 0.032 ± 0.002 U/mg protein in controls to 0.182 ± 0.002 U/mg in Group H. SOD activity followed a similar trend. Liver SOD levels increased from 0.030 ± 0.001 U/mg protein in Group A to 0.167 ± 0.002 U/mg protein in Group H, while kidney SOD rose from 0.38 ± 0.01 U/mg protein in controls to a peak of 4.38 ± 0.04 U/mg in Group H, reflecting pronounced antioxidant activation. Histopathological analyses revealed progressive hepatocellular degeneration, periportal inflammation, and vascular congestion, with Group H exhibiting hepatocellular vacuolation and necrosis. In kidneys, lesions ranged from glomerular atrophy and tubular necrosis in single exposures to extensive tubular damage and glomerular alterations in Group H. These findings underscore a dose-dependent and synergistic toxic interaction of these pesticides, warranting regulatory attention to mixture exposures. The study advocates integrating oxidative biomarkers and histopathological evaluations for comprehensive pesticide risk assessments.

Keywords: Oxidative Stress; Pesticide Mixtures; Organophosphates; Pyrethroids; Dichlorvos; Dimethoate; Cypermethrin; Liver Toxicity; Kidney Injury; Malondialdehyde (MDA); Superoxide Dismutase (SOD); Catalase (CAT).

1. Introduction

The extensive use of synthetic pesticides in agriculture has raised considerable concerns regarding their toxicological impact on human and animal health. Among the most widely applied are organophosphates and pyrethroids, which are frequently used either singly or in combination to control pests due to their broad-spectrum efficacy. Dichlorvos and dimethoate (organophosphates) act mainly by irreversibly inhibiting acetylcholinesterase, thereby disrupting neurotransmission, while cypermethrin (a pyrethroid) alters sodium channel kinetics, leading to sustained neuronal excitation [1,2]. Although their mechanisms differ, co-exposure is common in agricultural and domestic settings, raising the likelihood of additive or synergistic toxicity [3].

The liver and kidney, as primary detoxification and excretory organs, are particularly susceptible to pesticide-induced injury. Organophosphates and pyrethroids are well documented to trigger oxidative stress, characterised by overproduction of reactive oxygen species (ROS), lipid peroxidation, and subsequent alterations in antioxidant defence systems such as superoxide dismutase (SOD) and catalase (CAT) [4,5]. Lipid peroxidation, measured via malondialdehyde (MDA), is a reliable biomarker of oxidative damage, while perturbations in SOD and CAT activities reflect adaptive or overwhelmed antioxidant responses [6]. Persistent oxidative imbalance contributes to hepatocellular necrosis, vascular congestion, glomerular atrophy, and tubular degeneration, as frequently observed in histopathological studies of pesticide exposure [7].

Despite increasing knowledge of individual pesticide toxicodynamics, evidence on the combined effects of organophosphates and pyrethroids remains limited, even though such exposures reflect realistic environmental

conditions. Earlier reports suggest that binary and ternary mixtures exert more severe oxidative and histological alterations than single exposures, highlighting the risk of synergistic interactions [7,3]. Evaluating mixture toxicity is therefore critical for advancing environmental risk assessments and refining regulatory standards, as conventional single-compound evaluations may underestimate health risks.

In light of this, the present study investigates the subacute effects of dichlorvos, dimethoate, and cypermethrin, both individually and in combination, on oxidative stress biomarkers and histopathological architecture of rat liver and kidney following 28 days of exposure. By integrating biochemical and morphological assessments, this work provides comprehensive insights into the synergistic toxicity of pesticide mixtures and underscores the necessity of adopting mixture-based evaluations in toxicological risk assessment.

1.1. Study Objectives

The objectives of this study were to:

1. Evaluate the oxidative stress responses in female Wistar rats following 28-day exposure to dichlorvos, dimethoate, cypermethrin, and their combinations.

2. Quantify lipid peroxidation levels using malondialdehyde (MDA) as a biomarker of oxidative damage in liver and kidney tissues.

3. Assess the activity of key antioxidant enzymes—catalase (CAT) and superoxide dismutase (SOD)—as indicators of adaptive defence mechanisms.

4. Examine histopathological alterations in hepatic and renal tissues to establish structural evidence of pesticide-induced toxicity.

5. Compare the toxicological outcomes of single, binary, and ternary pesticide exposures to determine possible additive or synergistic interactions.

6. Provide integrated biochemical and histological insights to support pesticide risk assessment under realistic multi-pesticide exposure scenarios.

2. Materials and Methods

2.1. Chemicals and Reagents

Analytical-grade insecticides—dichlorvos, dimethoate, and cypermethrin—were obtained from certified commercial suppliers. All other reagents used in biochemical assays were of analytical grade and procured from standard laboratory suppliers.

2.2. Experimental Animals and Housing

Thirty-two adult female albino rats were obtained from a reputable animal breeding facility. The animals were housed in well-ventilated cages under standard laboratory conditions (12 h light/dark cycle, temperature 22–25 °C, relative humidity 50–60%) with free access to commercial pellet diet and water. They were acclimatised for seven days prior to commencement of the experiment.

2.3. Experimental Design and Treatment Protocol

Animals were randomly assigned into eight groups (n = 4 per group) as follows:

- **Group A (Control):** Exposed to water spray.
- **Group B:** Exposed to dichlorvos.
- **Group C:** Exposed to dimethoate.
- **Group D:** Exposed to cypermethrin.
- **Group E:** Exposed to dichlorvos and dimethoate.
- **Group F:** Exposed to dichlorvos and cypermethrin.
- **Group G:** Exposed to dimethoate and cypermethrin.
- **Group H:** Exposed to dichlorvos, dimethoate, and cypermethrin.

Solutions of the insecticides were prepared at a concentration of 1.33 mL/L, and spraying was performed at a dose rate of 0.05 mL/m². The animals were exposed once daily for 28 days. At the end of the exposure period, rats were anaesthetised and sacrificed for tissue and serum collection.

2.4. Biochemical Assays

2.4.1. Protein Concentration

Protein concentration in tissue homogenates was determined using the Biuret method [8]. The assay is based on the reaction of cupric ions in alkaline solution with peptide bonds to form a purple-coloured complex, the intensity of which was measured spectrophotometrically.

2.4.2. Malondialdehyde (MDA)

Lipid peroxidation was evaluated by determining malondialdehyde (MDA) levels using the thiobarbituric acid reactive substances (TBARS) method [9]. The red MDA–TBA adduct formed was quantified at 535 nm.

2.4.3. Superoxide Dismutase (SOD) Activity

D activity was assessed following Misra and Fridovich [10]. The method is based on the ability of SOD to inhibit the auto-oxidation of epinephrine at alkaline pH (10.2). The extent of inhibition was used as an index of enzyme activity.

2.4.4. Catalase Activity

Catalase activity was determined according to the method of Sinha [11]. In this assay, hydrogen peroxide decomposes in the presence of catalase, and the residual H_2O_2 reacts with dichromate-acetic acid to yield chromic acetate, which was quantified spectrophotometrically at 570–610 nm.

2.5. Histopathological Examination

Portions of liver and kidney tissues were excised and fixed in 10% buffered neutral formalin for 72 h at room temperature. The tissues were dehydrated in ascending grades of ethanol (70%, 90%, and 95%), cleared in xylene,

and embedded in paraffin wax (melting point 56 °C). Sections of 5 µm thickness were cut using a rotary microtome, mounted on egg albumin-coated slides, dewaxed, and hydrated through descending grades of ethanol. Staining was performed with 1% alcoholic eosin, followed by mounting in Canada balsam. Slides were examined under a Leitz DIALUX research microscope, and photomicrographs were captured at ×40 magnification [12].

3. Statistical Analysis

Data were expressed as mean ± standard error of mean (SEM). Statistical differences among groups were evaluated using one-way analysis of variance (ANOVA) followed by appropriate post hoc tests. A value of $p < 0.05$ was considered statistically significant.

4. Results

Figure 1 presents the malondialdehyde (MDA) concentrations in liver tissues of rats exposed to dichlorvos, dimethoate, cypermethrin, and their combinations over 28 days. Group A (control) recorded the lowest MDA level at approximately 3.2 nmol/g fresh weight, indicating baseline lipid peroxidation in the absence of pesticide exposure.

Exposure to individual pesticides resulted in significantly elevated MDA levels compared to control ($p < 0.05$). Group B (dichlorvos) showed an increase to 4.1 nmol/g, Group C (dimethoate) to 4.3 nmol/g, and Group D (cypermethrin) to 4.4 nmol/g, with Groups C and D not significantly different from each other but significantly higher than Group B ($p < 0.05$).

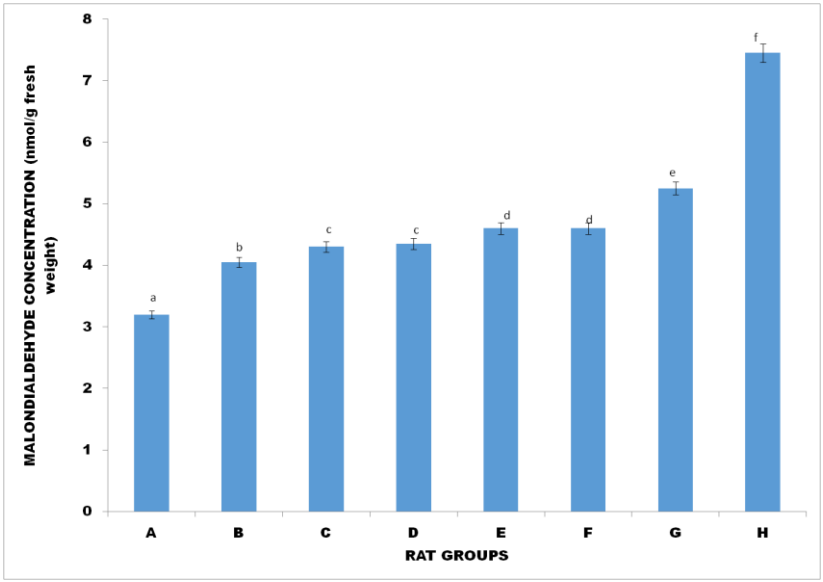

Figure 1. Malondialdehyde (MDA) Concentration in Liver of Rats Exposed to Dichlorvos, Dimethoate, Cypermethrin, and Their Combinations Over 28 Days. Calculated values are means of four determinations ± SEM. Bars bearing different alphabets are significantly different ($p<0.05$).

Binary combinations further amplified MDA concentrations. Group E (dichlorvos + dimethoate) and Group F (dichlorvos + cypermethrin) both recorded 4.7 nmol/g, which were significantly higher than Groups B, C, and D ($p < 0.05$) but not different from each other. Group G (dimethoate + cypermethrin) showed a more pronounced increase to 5.3 nmol/g, which was significantly higher than all previous groups ($p < 0.05$).

The highest MDA concentration was observed in Group H (dichlorvos + dimethoate + cypermethrin) at 7.5 nmol/g, which was significantly different from all other groups ($p < 0.05$), indicating the strongest lipid peroxidation and oxidative stress when all three pesticides were combined. This trend reflects a dose-dependent and interactive effect of pesticide exposure on hepatic oxidative damage.

Figure 2 illustrates the malondialdehyde (MDA) concentration in kidney tissues of rats following 28 days of exposure to dichlorvos, dimethoate, cypermethrin, and their combinations. The control group (A) recorded the lowest MDA level at approximately 2.9 nmol/g fresh weight, indicating normal renal oxidative status.

Exposure to dichlorvos (Group B) significantly increased the MDA concentration to 3.5 nmol/g ($p < 0.05$). Group C (dimethoate) showed a further increase to 4.3 nmol/g, which was significantly higher than Groups A and B. Group D (cypermethrin) recorded an MDA level of 4.9 nmol/g, significantly higher than Group C ($p < 0.05$), indicating a stronger oxidative impact in renal tissue.

Among the combination groups, Group E (dichlorvos + dimethoate) had an MDA value of 4.5 nmol/g, while Group F (dichlorvos + cypermethrin) showed 4.9 nmol/g. These were not significantly different from Group D, but were significantly higher than Groups B and C ($p < 0.05$). Group G (dimethoate + cypermethrin) recorded 4.5 nmol/g, similar to Group E, and significantly lower than Group F.

Group H, which received all three pesticides, showed the highest MDA level at approximately 7.3 nmol/g, significantly higher than all other groups ($p < 0.05$). This sharp rise suggests a cumulative or synergistic increase in renal lipid peroxidation due to the combined exposure to all three pesticides.

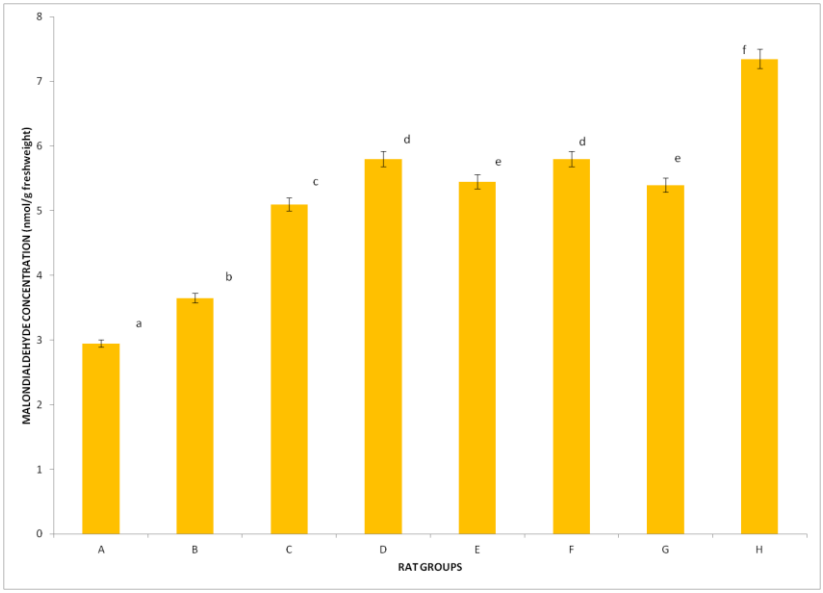

Figure 2. Malondialdehyde (MDA) Concentration in Kidney of Rats Exposed to Dichlorvos, Dimethoate, Cypermethrin, and Their Combinations Over 28 Days. Calculated values are means of four determinations ± SEM. Bars bearing different alphabets are significantly different ($p<0.05$).

Figure 3 presents the specific activity of catalase in liver tissues of rats exposed to dichlorvos, dimethoate, cypermethrin, and their combinations for 28 days. The data are expressed as mean ± SEM (n = 4), and bars bearing different superscript letters differ significantly ($p < 0.05$).

Groups A and B (control and dichlorvos-exposed) showed the lowest catalase activities at 0.045 ± 0.002 U/mg protein and 0.046 ± 0.002 U/mg protein, respectively, with no significant difference between them ($p > 0.05$). This indicates that dichlorvos alone did not significantly stimulate catalase activity compared to control.

Group C (dimethoate) showed a significant increase to 0.056 ± 0.001 U/mg protein, and Group D (cypermethrin) exhibited a further rise to 0.063 ± 0.001 U/mg protein, both significantly higher than Groups A and B ($p < 0.05$). Group E (dichlorvos + dimethoate) had 0.072 ± 0.002 U/mg protein, while Group F (dichlorvos + cypermethrin) showed 0.081 ± 0.002 U/mg protein, with both values significantly higher than their respective single exposure groups ($p < 0.05$).

Group G (dimethoate + cypermethrin) recorded 0.108 ± 0.002 U/mg protein, while the highest catalase activity was observed in Group H (triple combination) at 0.125 ± 0.002 U/mg protein, significantly higher than all other groups ($p < 0.05$). This progressive increase suggests that combined pesticide exposure enhanced the hepatic catalase response in a dose- and interaction-dependent manner, likely as a compensatory antioxidant mechanism.

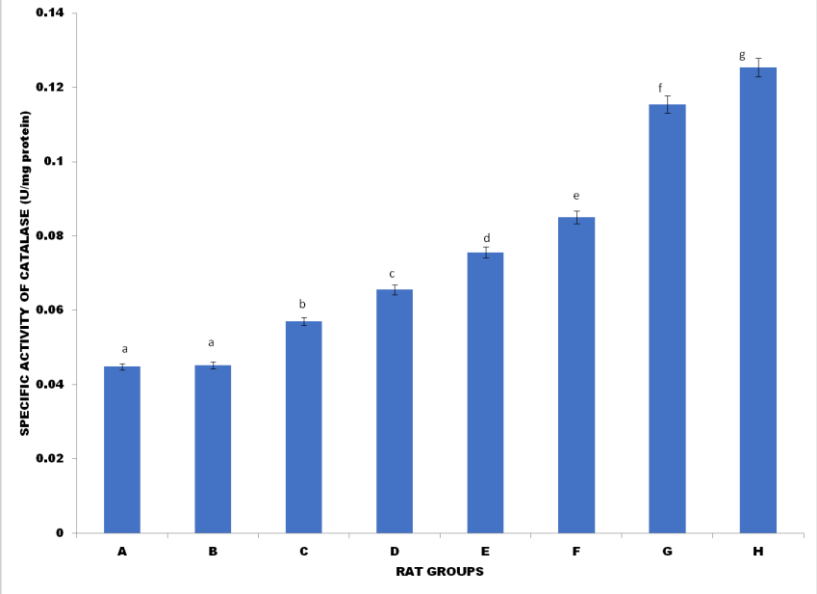

Figure 3. Catalase Specific Activity in Liver of Rats Exposed to Dichlorvos, Dimethoate, Cypermethrin, and Their Combinations Over 28 Days. Calculated values are means of four determinations ± SEM. Bars bearing different alphabets are significantly different ($p<0.05$).

Figure 4 presents the specific activity of catalase in the kidneys of rats following 28-day exposure to dichlorvos, dimethoate, cypermethrin, and their combinations. Values are expressed as mean ± SEM ($n = 4$), with significant differences denoted by different superscript letters ($p < 0.05$).

Group A (control) had the lowest catalase activity at 0.032 ± 0.002 U/mg protein, while Group B (dichlorvos) showed a slight but significant increase to 0.037 ± 0.001 U/mg protein ($p < 0.05$). Group C (dimethoate) recorded 0.051 ± 0.001 U/mg protein, significantly higher than both A and B. Group D (cypermethrin) further increased to 0.059 ± 0.001 U/mg protein, significantly greater than Group C ($p < 0.05$).

Among the binary combinations, Group E (dichlorvos + dimethoate) showed a substantial rise to 0.124 ± 0.002 U/mg protein, while Group F (dichlorvos + cypermethrin) recorded 0.128 ± 0.002 U/mg protein, both significantly

higher than Groups D and below ($p < 0.05$). Group G (dimethoate + cypermethrin) also maintained a similar activity at 0.131 ± 0.002 U/mg protein, not significantly different from E and F.

Group H (dichlorvos + dimethoate + cypermethrin) recorded the highest catalase activity at 0.182 ± 0.002 U/mg protein, significantly greater than all other groups ($p < 0.05$), indicating an amplified antioxidant enzyme response under combined pesticide stress.

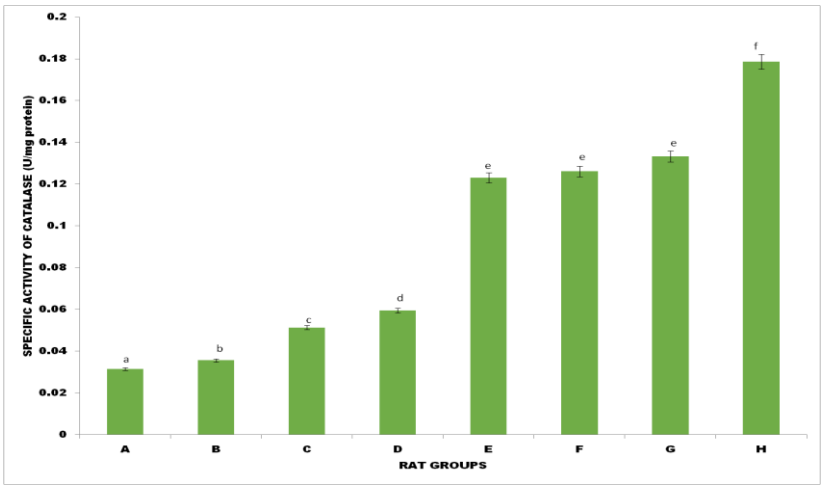

Figure 4. Catalase Specific Activity in Kidney of Rats Exposed to Dichlorvos, Dimethoate, Cypermethrin, and Their Combinations Over 28 Days. Calculated values are means of four determinations ± SEM. Bars bearing different alphabets are significantly different ($p<0.05$).

Figure 5 illustrates the specific activity of superoxide dismutase (SOD) in the liver tissues of rats exposed to dichlorvos, dimethoate, cypermethrin, and their combinations over a 28-day period. Data are presented as mean ± SEM for four determinations, with statistically significant differences indicated by different superscript letters ($p < 0.05$).

Group A (control) showed the lowest SOD activity at 0.030 ± 0.001 U/mg protein. Group B (dichlorvos) had a modest but significant increase to 0.039 ± 0.001 U/mg protein ($p < 0.05$). Group C (dimethoate) showed a further significant elevation to 0.056 ± 0.001 U/mg protein, while Group D (cypermethrin) recorded 0.035 ± 0.001 U/mg protein, which was significantly lower than Group C ($p < 0.05$).

In the binary combination groups, Group E (dichlorvos + dimethoate) and Group F (dichlorvos + cypermethrin) each showed SOD activities of 0.086 ± 0.002 U/mg protein, significantly higher than their respective single-exposure counterparts ($p < 0.05$). Group G (dimethoate + cypermethrin) recorded 0.112 ± 0.002 U/mg protein, significantly higher than all previous groups ($p < 0.05$).

The highest SOD activity was observed in Group H (triple combination), which reached 0.167 ± 0.002 U/mg protein, significantly exceeding all other groups ($p < 0.05$). This upward trend suggests a dose-responsive and synergistic activation of the antioxidant defense system under increasing pesticide burden.

Figure 6 shows the specific activity of superoxide dismutase (SOD) in the kidneys of rats exposed to dichlorvos, dimethoate, cypermethrin, and their combinations over a 28-day period. Values are expressed as mean ± SEM ($n = 4$), and bars marked with different superscript letters differ significantly ($p < 0.05$).

Group A (control) recorded the lowest SOD activity at 0.38 ± 0.01 U/mg protein. Group B (dichlorvos) showed a significant increase to 1.20 ± 0.02 U/mg protein, while Group C (dimethoate) rose further to 1.84 ± 0.02 U/mg protein, both significantly higher than the control ($p < 0.05$). Group D (cypermethrin) recorded 2.23 ± 0.03 U/mg protein, significantly higher than Group C ($p < 0.05$).

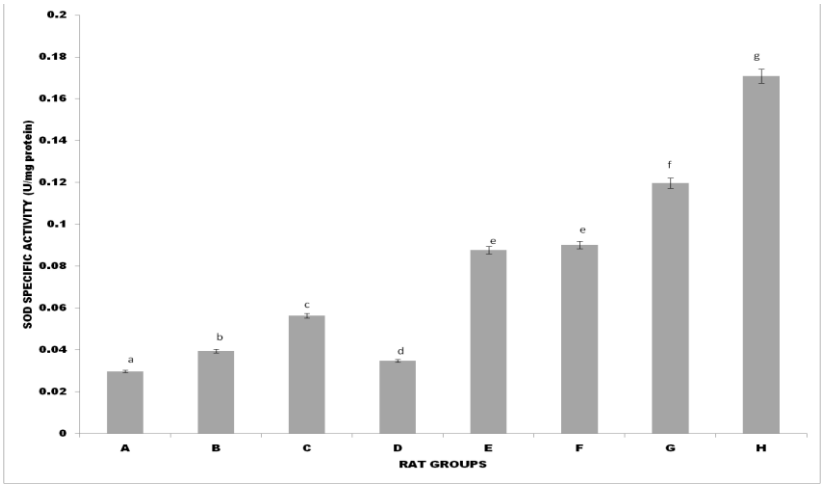

Figure 5. Superoxide dismutase (SOD) Specific Activity in Liver of Rats Exposed to Dichlorvos, Dimethoate, Cypermethrin, and Their Combinations Over 28 Days. Calculated values are means of four determinations ± SEM. Bars bearing different alphabets are significantly different ($p<0.05$).

In the binary exposure groups, SOD activity continued to rise. Group E (dichlorvos + dimethoate) showed 2.48 ± 0.02 U/mg protein, Group F (dichlorvos + cypermethrin) recorded 2.63 ± 0.02 U/mg protein, and Group G (dimethoate + cypermethrin) exhibited 2.79 ± 0.03 U/mg protein, all significantly higher than single exposure groups ($p < 0.05$).

The highest SOD activity was found in Group H (triple combination), with 4.38 ± 0.04 U/mg protein, significantly higher than all other groups ($p < 0.05$), suggesting a potent antioxidant response triggered by cumulative oxidative stress from combined pesticide exposure.

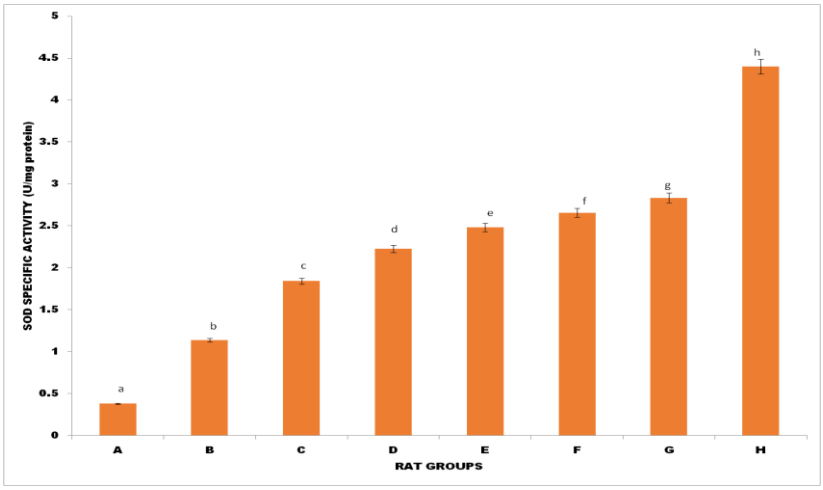

Figure 6. Superoxide dismutase (SOD) Specific Activity in Kidney of Rats Exposed to Dichlorvos, Dimethoate, Cypermethrin, and Their Combinations Over 28 Days. Calculated values are means of four determinations ± SEM. Bars bearing different alphabets are significantly different ($p<0.05$).

Plates 1–16 present photomicrographs of liver and kidney tissues from the experimental groups, illustrating histopathological outcomes following 28-day pesticide exposure. Plates 1 and 9 depict the control groups for liver and kidney respectively, showing preserved histological architecture with intact hepatocytes, glomeruli, and renal tubules. In contrast, progressive pathological changes such as periportal inflammation, vascular congestion, hepatocellular vacuolation, necrosis, glomerular atrophy, tubular vacuolation, and interstitial haemorrhage were evident in treated groups. The alterations were mild under single exposures but became more severe with binary and ternary combinations. The most extensive lesions, including hepatocellular degeneration and widespread tubular necrosis, occurred in the triple-exposure groups (Plates 8 and 16), underscoring the synergistic toxic impact of multiple pesticide exposures on vital organs.

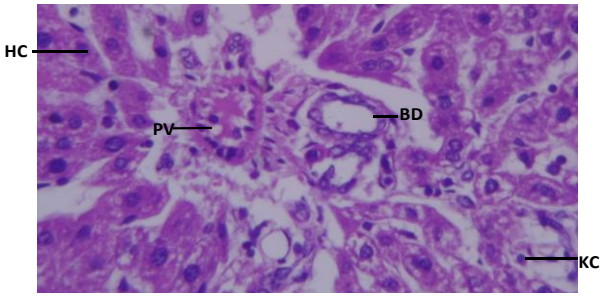

Plate 1. Photomicrograph of Liver Tissue from Control Group (Group A) Showing Normal Histological Architecture. **Legend (H&E, ×400):** HC – Hepatocytes; PV – Portal Vein; BD – Bile Duct; KC – Kupffer Cells. No visible pathological alterations observed.

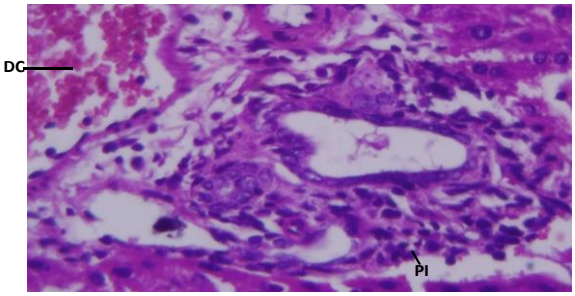

Plate 2. Photomicrograph of Liver Tissue from Group B Rats Exposed to Dichlorvos Showing Periportal Inflammation. Legend (H&E, ×400): DC – Degenerating Cells; PI – Periportal Infiltration of Inflammatory Cells. Histopathological features indicate hepatic inflammation and early cellular damage associated with dichlorvos exposure.

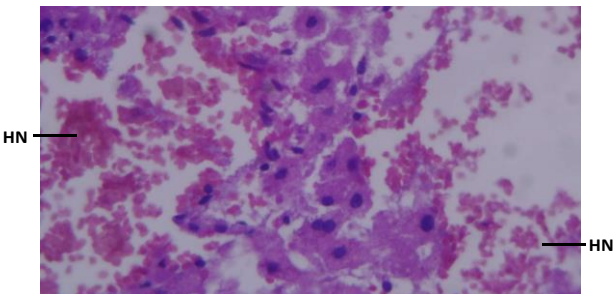

Plate 3. Photomicrograph of Liver Tissue from Group C Rats Exposed to Dimethoate Showing Hemorrhagic Necrosis. Legend (H&E, ×400): HN – Hemorrhagic Necrosis. The presence of necrotic foci and dense inflammatory cell infiltration indicates significant hepatocellular injury induced by dimethoate exposure.

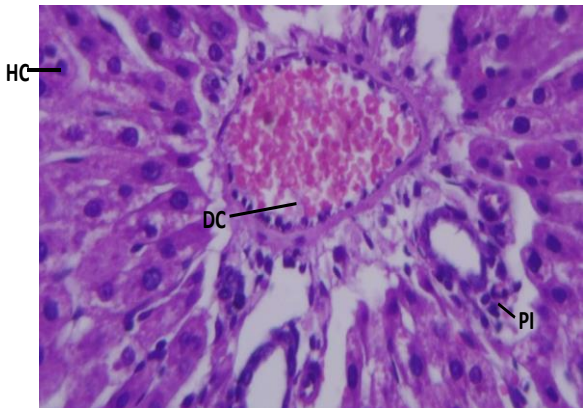

Plate 4. Photomicrograph of Liver Tissue from Group D Rats Exposed to Cypermethrin Showing Congested Central Vein and Mild Hepatocellular Disarray. Legend (H&E, ×400): The image reveals a prominent congested central vein surrounded by hepatocytes exhibiting mild structural alteration, suggestive of early vascular and parenchymal stress due to cypermethrin exposure.

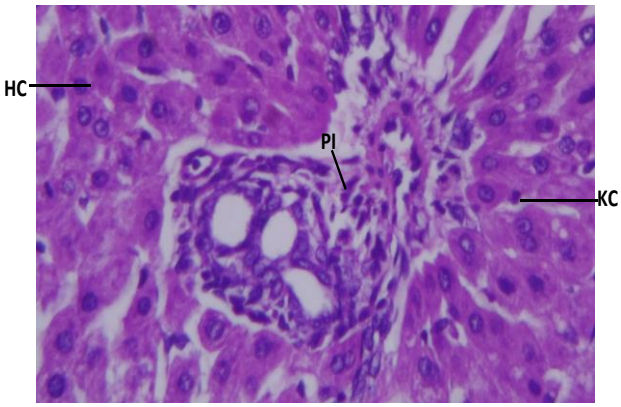

Plate 5. Photomicrograph of Liver Tissue from Group E Rats Exposed to Dichlorvos and Dimethoate Showing Periportal Infiltration of Inflammatory Cells. Legend (H&E, ×400): HC – Hepatocytes; PI – Periportal Infiltration; KC – Kupffer Cells. The image reveals clear evidence of periportal inflammatory cell infiltration, indicating an active immune response and hepatic inflammation resulting from combined pesticide exposure.

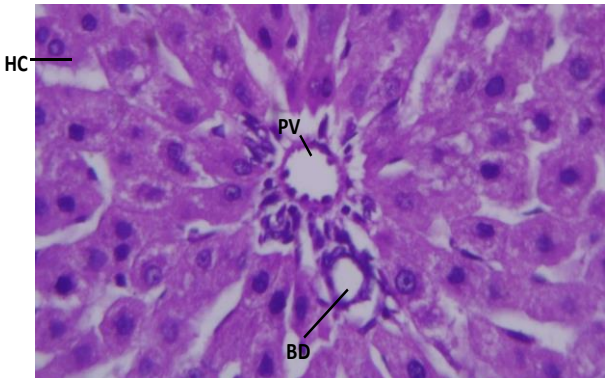

Plate 6. Photomicrograph of Liver Tissue from Group F Rats Exposed to Dichlorvos and Cypermethrin Showing Mild Portal Inflammation and Preserved Hepatic Architecture. Legend (H&E, ×400): HC – Hepatocytes; PV – Portal Vein; BD – Bile Duct. The portal area appears mildly inflamed with some cellular infiltration, but the surrounding hepatocytes maintain a generally preserved structure, indicating a moderate hepatic response to dual pesticide exposure.

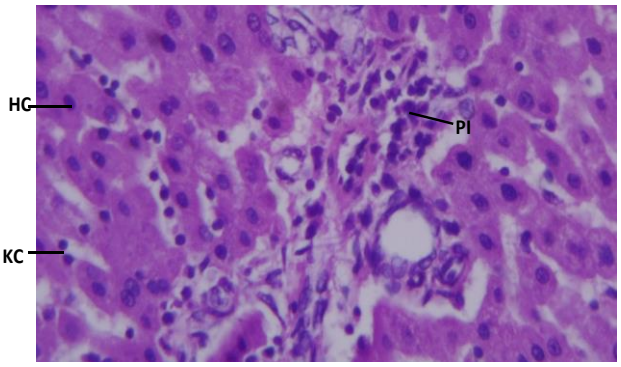

Plate 7. Photomicrograph of Liver Tissue from Group G Rats Exposed to Dimethoate and Cypermethrin Showing Marked Periportal Infiltration and Hepatocellular Disruption. Legend (H&E, ×400): HC – Hepatocytes; KC – Kupffer Cells; PI – Periportal Infiltration. The section reveals pronounced infiltration of inflammatory cells around the portal area, along with signs of hepatocellular alteration, suggesting a strong hepatic inflammatory response to the combined pesticide exposure.

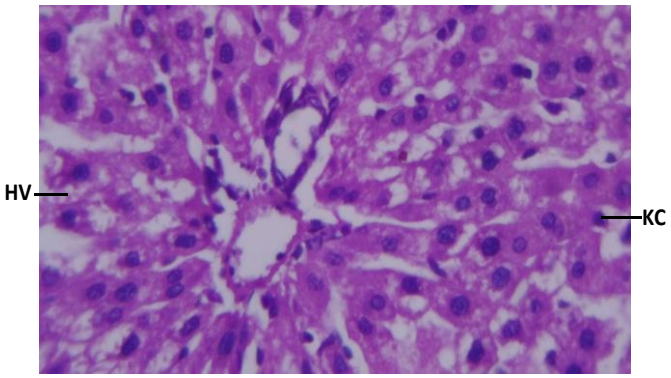

Plate 8. Photomicrograph of Liver Tissue from Group H Rats Exposed to Dichlorvos, Dimethoate, and Cypermethrin Showing Hepatocellular Degeneration and Vascular Congestion. Legend (H&E, ×400): HV – Hepatic Vessel; KC – Kupffer Cells. The image reveals a congested hepatic vessel with surrounding hepatocytes exhibiting signs of cytoplasmic vacuolation and disruption, indicative of cumulative toxic stress from triple pesticide exposure.

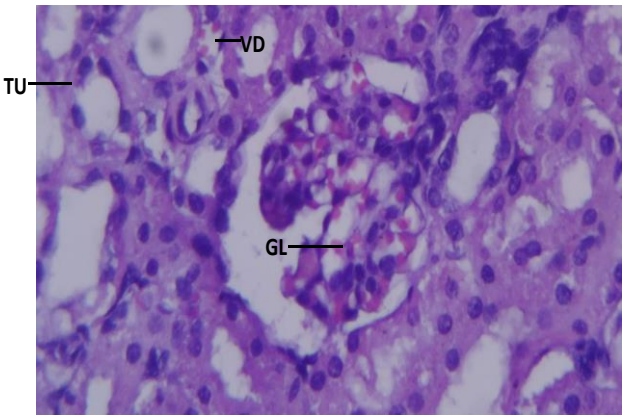

Plate 9. Photomicrograph of Kidney Tissue from Control Group (Group A) Showing Normal Renal Histoarchitecture. Legend (H&E, ×400): TU – Tubules; GL – Glomerulus; VD – Vascular Domain. The section demonstrates intact renal structures with normal glomerular morphology, patent vascular domains, and well-organized renal tubules, indicating no pathological alteration.

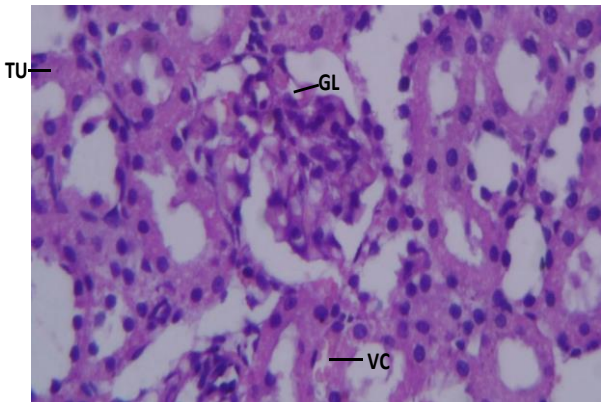

Plate 10. Photomicrograph of Kidney Tissue from Group B Rats Exposed to Dichlorvos Showing Glomerular Atrophy and Tubular Vacuolation. Legend (H&E, ×400): TU – Tubules; GL – Glomerulus; VC – Vacuolated Cells. The renal tissue exhibits glomerular shrinkage and marked cytoplasmic vacuolation within tubular epithelium, indicating nephrotoxic effects associated with dichlorvos exposure.

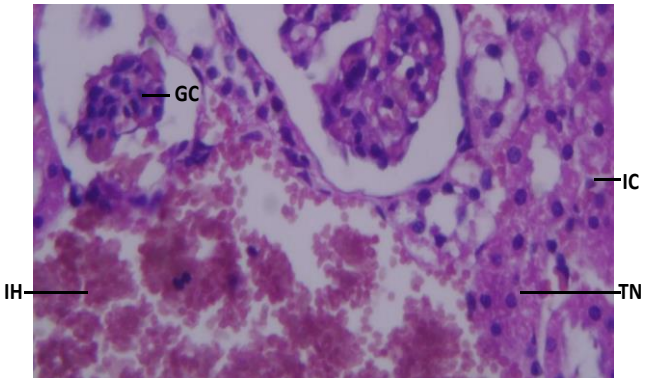

Plate 11. Photomicrograph of Kidney Tissue from Group C Rats Exposed to Dimethoate Showing Inflammatory Cell Infiltration and Glomerular Congestion. Legend (H&E, ×400): GC – Glomerular Congestion; IH – Interstitial Hemorrhage; IC – Interstitial Congestion; TN – Tubular Necrosis. The section reveals pronounced glomerular vascular congestion, diffuse inflammatory infiltration, interstitial hemorrhage, and signs of necrosis, indicating significant nephrotoxicity induced by dimethoate exposure.

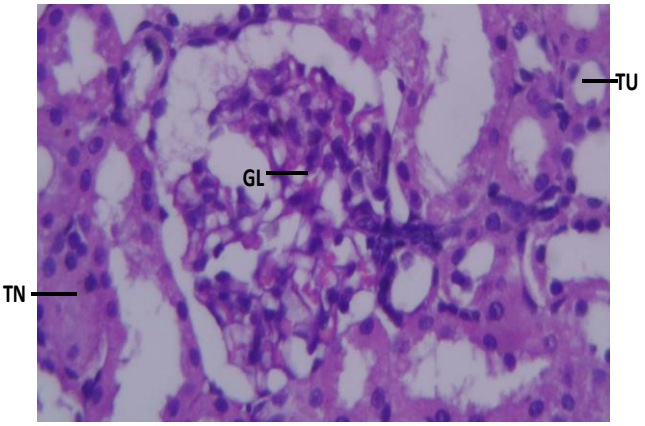

Plate 12. Photomicrograph of Kidney Tissue from Group D Rats Exposed to Cypermethrin Showing Focal Tubular Necrosis with Preserved Glomeruli and Tubular Structures. Legend (H&E, ×400): TN – Tubular Necrosis; GL – Glomerulus; TU – Tubules. The image reveals localized necrosis in tubular epithelium, while the glomeruli and most renal tubules retain normal histoarchitecture, indicating mild but focal nephrotoxic effects of cypermethrin.

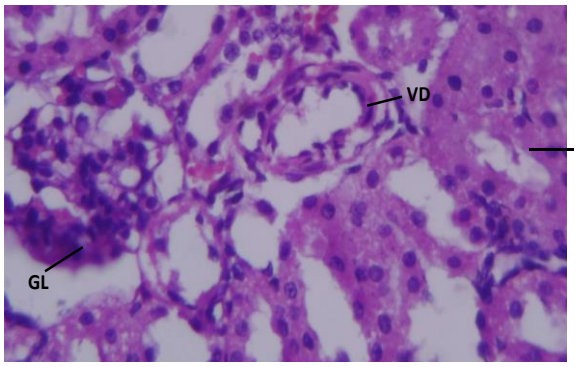

Plate 13. Photomicrograph of Kidney Tissue from Group E Rats Exposed to Dichlorvos and Dimethoate Showing Interstitial Vasodilatation with Preserved Tubular and Glomerular Structures. Legend (H&E, ×400): GL – Glomerulus; TU – Tubules; VD – Vasodilatation. The renal tissue exhibits normal histological appearance of glomeruli and renal tubules, alongside noticeable vasodilatation in the interstitial space, suggesting vascular response to combined pesticide exposure.

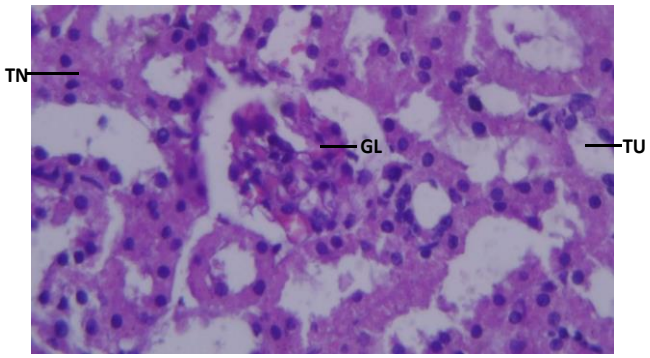

Plate 14. Photomicrograph of Kidney Tissue from Group F Rats Exposed to Dichlorvos and Cypermethrin Showing Tubular Necrosis and Intact Glomeruli. Legend (H&E, ×400): TN – Tubular Necrosis; GL – Glomerulus; TU – Tubules. The image shows degenerative changes in the tubular epithelium, particularly focal necrosis, while the glomeruli and most renal tubules retain their structural integrity, suggesting subacute nephrotoxicity from combined pesticide exposure.

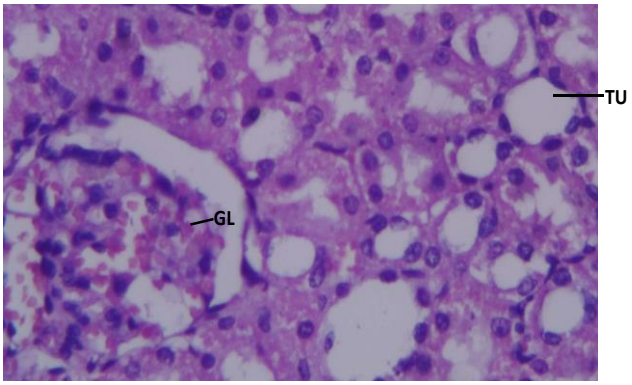

Plate 15. Photomicrograph of Kidney Tissue from Group G Rats Exposed to Dimethoate and Cypermethrin Showing Glomerular Congestion and Tubular Degeneration. Legend (H&E, ×400): GL – Glomerulus; TU – Tubules. The glomerulus appears congested with erythrocyte accumulation, while several renal tubules exhibit cytoplasmic vacuolation and degeneration, suggesting moderate nephrotoxic effects from the pesticide combination.

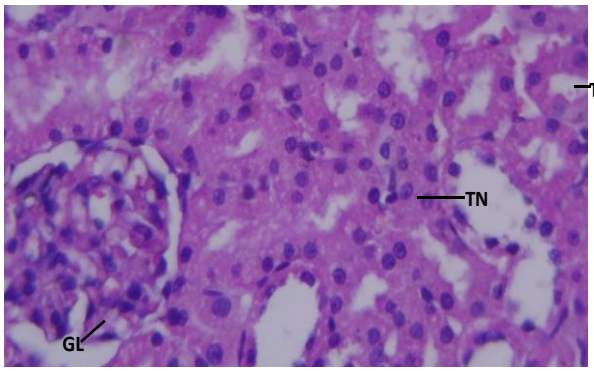

Plate 16. Photomicrograph of Kidney Tissue from Group H Rats Exposed to Dichlorvos, Dimethoate, and Cypermethrin Showing Extensive Tubular Necrosis and Glomerular Alterations. Legend (H&E, ×400): GL – Glomerulus; TN – Tubular Necrosis; TU – Tubules. The section reveals marked tubular necrosis and early glomerular distortion, indicating severe nephrotoxic damage due to combined exposure to all three pesticides.

5. Discussion

The patterns of oxidative stress biomarkers presented in Figures 1–6 collectively illustrate a consistent trend of pesticide-induced oxidative perturbations in hepatic and renal tissues. The marked elevation of malondialdehyde (MDA) levels in both liver and kidney tissues in treated groups, especially with binary and ternary combinations, confirms the pro-oxidant properties of dichlorvos, dimethoate, and cypermethrin. MDA is a well-established end-product of lipid peroxidation and is commonly used to reflect the extent of membrane damage under oxidative stress. The increases observed across treatment groups suggest progressive lipid peroxidation and compromise of membrane integrity, particularly under multi-pesticide exposures, a finding supported by previous studies that reported synergistic oxidative toxicity when organophosphates and pyrethroids are combined [6,3].

Concomitant with lipid peroxidation, the activities of antioxidant enzymes—catalase (CAT) and superoxide dismutase (SOD)—were significantly upregulated, particularly in groups exposed to combined pesticides. The rising activities of CAT and SOD in both liver and kidney tissues likely represent an adaptive cellular response to counteract the excessive generation of reactive oxygen species (ROS). Catalase catalyzes the decomposition of hydrogen peroxide to water and oxygen, while SOD catalyzes the dismutation of superoxide radicals into less reactive species. The observed upregulation is consistent with studies showing enhanced antioxidant enzyme expression in response to xenobiotic-induced oxidative stress [5,7].

Interestingly, the extent of enzyme elevation was more pronounced in the kidney than the liver, especially for SOD activity, suggesting that renal tissues may be more metabolically responsive—or perhaps more vulnerable—to oxidative injury under these exposure conditions. This observation aligns with earlier toxicological reports where kidneys, due to their high blood flow and active excretory roles, accumulate toxins and demonstrate heightened oxidative responses [2,4]. Moreover, the synergistic toxicity indicated by the pronounced biochemical alterations in triple-exposure groups underscores the importance of evaluating pesticide mixtures rather than single compounds, reflecting realistic environmental exposure scenarios.

Collectively, these findings reinforce the oxidative mechanism underlying pesticide toxicity and suggest a dose-dependent and interaction-sensitive disruption of redox balance. The simultaneous elevation of both lipid

peroxidation and antioxidant enzymes suggests an overwhelmed but reactive defence system. If such oxidative stress persists, it may culminate in tissue injury, apoptosis, or necrosis. Thus, regular monitoring of oxidative biomarkers and regulation of combined pesticide usage are essential to mitigate systemic toxicity and organ damage in exposed populations.

The histopathological examination of liver tissues across experimental groups reveals a progressive trend of hepatic damage corresponding to the type and combination of pesticide exposures. Group A, which served as the control, showed preserved hepatic architecture, providing a baseline for comparison. As pesticide exposure intensified across the groups—from single to multiple agents—the liver histology increasingly exhibited signs of cellular stress and inflammation. This trend is consistent with previous studies reporting that organophosphate (e.g., dichlorvos and dimethoate) and pyrethroid (e.g., cypermethrin) insecticides disrupt hepatic cellular homeostasis primarily via oxidative stress mechanisms and inflammatory responses [2,4].

The presence of periportal infiltration, congested hepatic vessels, hepatocellular disarray, and necrotic changes observed in various plates aligns with well-documented mechanisms of pesticide-induced hepatotoxicity. These pathological features are indicative of hepatic inflammation and oxidative damage, likely mediated by excessive production of reactive oxygen species (ROS) and lipid peroxidation [5]. In particular, dichlorvos and dimethoate, both cholinesterase inhibitors, are known to compromise mitochondrial integrity and induce lysosomal enzyme release, exacerbating tissue injury [7]. Moreover, cypermethrin has been shown to increase membrane permeability and lipid peroxidation in hepatic cells, further contributing to liver dysfunction [6].

Notably, the combination of pesticides (as seen in Groups E to H) resulted in more severe histological alterations compared to single-agent exposures. This suggests possible synergistic or additive toxic interactions among these chemicals. Such interactions can intensify hepatotoxic outcomes due to overlapping metabolic pathways and compounded oxidative burden [1]. For instance, combined organophosphate and pyrethroid exposure has been shown to inhibit antioxidant enzymes such as catalase and glutathione peroxidase, amplifying tissue vulnerability to oxidative injury [3].

The Kupffer cell activation noted in some sections is also significant. Kupffer cells, as resident macrophages of the liver, respond to xenobiotic insults by producing pro-inflammatory cytokines, which can perpetuate hepatic inflammation and fibrosis if the exposure is chronic or intense [13]. The progression of lesions observed in Plate 4.8 (Group H) reflects such compounded damage, underscoring the heightened risk posed by combined pesticide exposures under real-world environmental and occupational settings.

The histopathological evidence from Plates 1–8 substantiates the hepatotoxic potential of dichlorvos, dimethoate, and cypermethrin, both individually and in combination. The observed lesions highlight the relevance of exposure intensity, duration, and chemical interactions in determining hepatic outcomes. These findings support the need for stringent pesticide regulation and the incorporation of mixture toxicity in risk assessment models, especially in developing regions where exposure scenarios often involve multiple agrochemicals.

The histopathological evaluation of kidney tissues from Plates 9 to 16 reveals varying degrees of renal injury associated with exposure to dichlorvos, dimethoate, cypermethrin, and their combinations. In the control group

(Plate 9), normal renal histoarchitecture was observed, including intact glomeruli, well-defined tubular epithelial cells, and clear vascular domains, indicating physiological homeostasis in the absence of toxic insult. However, progressive degenerative changes in the renal microstructure were evident in groups exposed to one or more pesticides, in line with increasing toxic burden and oxidative disruption of renal tissues.

Exposure to dichlorvos alone (Plate 10) led to glomerular atrophy and prominent vacuolation of the tubular epithelium, features suggestive of nephrotoxicity. Organophosphates like dichlorvos are known to impair mitochondrial oxidative phosphorylation and induce lipid peroxidation in renal tubular cells, leading to loss of membrane integrity and vacuolar degeneration [7].

Dimethoate exposure (Plate 11) exacerbated renal damage, with evidence of glomerular congestion, inflammatory infiltration, and interstitial hemorrhage, indicating both vascular and cellular injury. These pathological changes reflect the compound's potential to elicit immune-mediated renal inflammation and oxidative stress, in agreement with previous reports [4].

Notably, cypermethrin exposure (Plate 12) produced focal tubular necrosis with preserved glomeruli, suggesting that pyrethroids may primarily target the tubular epithelium while sparing glomerular architecture in subacute conditions. Cypermethrin has been shown to cause mitochondrial swelling, increased malondialdehyde levels, and disruption of Na^+/K^+-ATPase in renal tubules, thereby initiating localized necrosis [6]. The co-exposure groups (Plates 13–16) demonstrated compounded pathology. Plate 13 (Group E: dichlorvos + dimethoate) presented relatively preserved glomeruli and tubules with interstitial vasodilatation, possibly reflecting early hemodynamic alterations without overt cellular degeneration. This may indicate a compensatory vascular response before the onset of irreversible damage.

However, rats exposed to dichlorvos and cypermethrin (Plate 14) showed distinct tubular necrosis, while those exposed to dimethoate and cypermethrin (Plate 15) exhibited glomerular congestion and marked tubular degeneration. These findings suggest additive or synergistic nephrotoxic effects when organophosphates and pyrethroids are combined, aligning with the reports that combined pesticide exposure enhances renal oxidative stress and suppresses key antioxidant enzymes such as catalase and superoxide dismutase [3,1].

The most pronounced lesions were seen in Plate 16 (Group H: exposed to all three pesticides), where widespread tubular necrosis and early glomerular alterations were evident. This confirms that multiple pesticide exposure acts cumulatively to impair renal function through overlapping pathways involving oxidative damage, inflammation, and vascular dysfunction [5]. The observed pathology corroborates with biochemical findings in similar studies, where elevated serum creatinine and urea levels paralleled histological evidence of tubular injury and glomerular damage [2].

Plates 9–16 illustrate a clear dose-dependent and interaction-sensitive spectrum of pesticide-induced nephrotoxicity. While individual pesticides cause distinct patterns of renal injury, combined exposures produce compounded effects marked by vascular congestion, glomerular atrophy, tubular necrosis, and inflammatory infiltration. These findings underscore the renal vulnerability to xenobiotics and the need for integrated pesticide risk assessment frameworks that consider real-world.

6. Conclusion

In conclusion this study clearly demonstrates that exposure to dichlorvos, dimethoate, cypermethrin, and their combinations induces significant oxidative stress and histopathological damage in the liver and kidney tissues of rats. The elevated levels of malondialdehyde (MDA) observed in both organs indicate enhanced lipid peroxidation, while the corresponding increases in catalase (CAT) and superoxide dismutase (SOD) activities reflect compensatory antioxidant responses aimed at mitigating reactive oxygen species (ROS) overload.

Histological examinations further corroborate the biochemical findings, revealing progressive cellular degeneration, inflammatory infiltration, vascular congestion, and necrosis, particularly in groups exposed to multiple pesticides. Notably, the most severe alterations occurred in the group exposed to the triple combination, suggesting a synergistic or additive toxic effect.

Overall, the results underscore the potential health risks associated with single and especially combined pesticide exposures. These findings highlight the need for stricter regulation of pesticide use, with particular attention to the real-world scenario of multi-pesticide exposure. Furthermore, the integration of oxidative stress biomarkers and histopathological assessments provides a reliable approach for evaluating pesticide-induced organ toxicity.

7. Future Suggestions

To strengthen knowledge on pesticide mixture toxicity and guide regulatory frameworks, future research should:

1. Extend exposure duration beyond 28 days to evaluate chronic and cumulative effects on liver and kidney function.

2. Incorporate additional biomarkers of oxidative stress, inflammation, and apoptosis for a broader mechanistic understanding.

3. Investigate other vital organs such as the brain, lungs, and reproductive system to assess systemic implications.

4. Explore potential protective roles of natural antioxidants, nutraceuticals, or phytochemicals against pesticide-induced oxidative injury.

5. Conduct dose–response and recovery studies to establish safe thresholds and the possibility of reversibility of damage.

6. Translate findings through field-based studies and epidemiological surveys to validate laboratory results under real-life exposure conditions.

Declarations

Source of Funding

This study received no specific grant from any funding agency in the public, commercial, or not-for-profit sectors.

Competing Interests Statement

The authors declare that they have no competing interests related to this work.

Consent for publication

The authors declare that they consented to the publication of this study.

Authors' contributions

Both the authors took part in literature review, analysis, and manuscript writing equally.

Availability of data and materials

Supplementary information is available from the authors upon reasonable request.

Institutional Review Board Statement

Not applicable for this study.

Informed Consent

Not applicable for this study.

References

[1] Sharma, A., Kumar, V., Thukral, A.K., Bhardwaj, R., & Shahzad, B. (2020). Review on organophosphate pesticide toxicity and its mechanism. Environ Nanotechnol Monit Manag., 14: 100333. https://doi.org/10.1016/j.enmm.2020.100333.

[2] Elsharkawy, E.R., Abd-Elkareem, M., & Althobaiti, F. (2021). Histopathological and biochemical alterations induced by dichlorvos in the liver and kidney of male rats. Saudi J Biol Sci., 28(4): 2267–2273. https://doi.org/10.1016/j.sjbs.2021.02.029.

[3] Khan, M.F., Shukla, R.K., & Dwivedi, N. (2022). Synergistic toxicity of pesticides in liver and kidney: A comprehensive review. Environ Toxicol Pharmacol., 96: 104004. https://doi.org/10.1016/j.etap.2022.104004.

[4] Abdel-Daim, M.M., Abd El-Aziz, T.H., Hassan, A.M., & Abushouk, A.I. (2020). Oxidative stress and inflammation induced by organophosphates: Mechanisms and protective strategies. Environ Sci Pollut Res., 27 (34): 42635–42652. https://doi.org/10.1007/s11356-020-09907-7.

[5] Anand, S., Srivastava, A., & Singh, V. (2022). Mechanistic insights into pesticide-induced oxidative stress and liver injury: Therapeutic roles of natural antioxidants. Chem Biol Interact., 357: 109889. https://doi.org/10.1016/j.cbi.2022.109889.

[6] Ali, S., Akhtar, N., Tabassum, S., & Khalid, S. (2023). Cypermethrin-induced biochemical and histopathological alterations in rat liver and kidney and the protective role of vitamin C. Toxicol Rep., 10: 456–464. https://doi.org/10.1016/j.toxrep.2023.01.045.

[7] Mossa, A.T.H., Mohafrash, S.M.M., & Abou-Taleb, H.K. (2021). Comparative toxicity of some insecticides on biochemical and histopathological alterations in rats. J King Saud Univ Sci., 33(3): 101304. https://doi.org/10.1016/j.jksus.2020.101304.

[8] Gornall, A.G., Bardawill, C.J., & David, M.M. (1949). Determination of serum proteins by means of the biuret reaction. J Biol Chem., 177(2): 751–766. https://doi.org/10.1016/S0021-9258(18)57021-5.

[9] Bird, R.P., Draper, H.H., & Hadley, M. (1982). Analysis of malondialdehyde in biological fluids. Methods Enzymol., 105: 293–305. https://doi.org/10.1016/0076-6879(84)05038-2.

[10] Misra, H.P., & Fridovich, I. (1972). The role of superoxide anion in the autoxidation of epinephrine and a simple assay for superoxide dismutase. J Biol Chem., 247(10): 3170–3175. https://doi.org/10.1016/s0021-9258(19)45228-9.

[11] Sinha, A.K. (1971). Colorimetric assay of catalase. Anal Biochem., 47(2): 389–394. https://doi.org/10.1016/0003-2697(71)90451-4.

[12] Drury, R.A.B., & Wallington, E.A. (1973). Carleton's histological technique (4th Edition). Oxford University Press.

[13] Gao, B., Jeong, W.I., & Tian, Z. (2020). Liver: The largest immunological organ and a site for tolerogenic immune responses. Cell Mol Immunol., 17(12): 1172–1181. https://doi.org/10.1038/s41423-020-00583-9.